THE ULTRASONIC IMPULSE RESPONSE OF UNIDIRECTIONAL CARBON FIBRE LAMINATES

L.P.Scudder(1), D.A.Hutchins(1) and J.T.Mottram(1)

(1) Engineering Department, Warwick University, Gibbet Hill Rd., Coventry, CV4 7AL.

1. INTRODUCTION

The generation of ultrasound by lasers was first demonstrated [1,2] soon after the invention of the laser itself. Subsequent experimental and theoretical work led to the emergence of laser ultrasound as a laboratory tool, a development that has been the subject of several reviews [3,4]. The potential virtues of the laser ultrasonic technique are its ability to generate broadband short duration pulses using a small source aperture without contact, leading to a system which can be modelled theoretically. A range of ultrasonic modes tend to be generated simultaneously (e.g. longitudinal, shear, surface and guided modes), although schemes exist for attempting to optimise the amplitude of a particular mode by changing the dimensions and shape of the beam at the irradiated surface, or by scanning the beam. A limitation of the technique is that the surface of a solid sample could be damaged, and it is higher in cost and generates lower amplitude ultrasonic waves compared to conventional piezoelectric ultrasonic transducers. Despite these limitations, the laser ultrasound technique has been used to investigate ultrasonic propagation in conventional and new engineering materials [4].

In this paper, the laser generation technique is used to generate a point impulse force on the surface of a carbon fibre reinforced polymer (CFRP) laminate. The resulting ultrasonic propagation is then examined to understand how acoustic emission transients, caused by growing defects, will propagate in composites, and follows on from the work of previous authors [5-7] to characterise the material quantitatively.

2. THEORETICAL BACKGROUND

The general theory [8] of single frequency, plane wave ultrasonic propagation in homogenous, anisotropic materials has proved adequate for interpreting our experimental data, and its results are outlined below. To ensure that elastic constant (C_{ij}) values utilised by the model are in the simplest form possible, the co-ordinate axes defining the wave propagation direction are coincident with the principal symmetry axes of the material, as shown in Fig.1. The theory combines Hooke's and Newton's laws to give the anisotropic wave equation. Substituting a plane wave solution into this yields three simultaneous

ULTRASONIC IMPULSE RESPONSE OF CARBON FIBRE LAMINATES

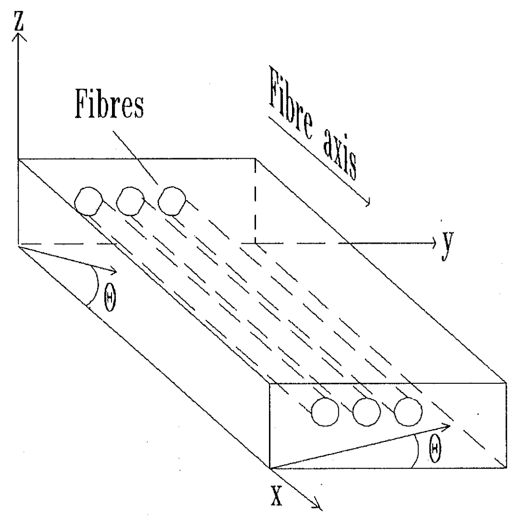

Fig. 1 Orientation of sample with respect to direction of wave propagation.

equations for the amplitude components of the wave. Wave velocities giving non-zero wave amplitudes can be found from the characteristic equation derived from the simultaneous equations coefficient determinant. In general three solutions for bulk wave velocity are found. For unidirectional carbon fibre , which belongs to the orthotropic symmetry class, two solutions for the longitudinal (L) and one of the shear modes (S1) have the form.

$$V_{L(S1)} = \sqrt{\frac{G \pm H}{2\rho}} \quad . \tag{1}$$

In the xz plane of an orthotropic material

$$G=(C_{11}Cos^2\theta+C_{33}Sin^2\theta+C_{55}) \ , \ H=\sqrt{[(C_{11}-C_{55})Cos^2\theta-(C_{33}-C_{55})Sin^2\theta]^2+Sin^2 2\theta(C_{13}+C_{55})^2}$$

and in the yz plane

$$G=(C_{22}Cos^2\theta+C_{33}Sin^2\theta+C_{44}) \ , \ H=\sqrt{[(C_{22}-C_{44})Cos^2\theta-(C_{33}-C_{44})Sin^2\theta]^2+Sin^2 2\theta(C_{23}+C_{44})^2}.$$

Where θ is the direction of propagation in the xz or yz planes. These solutions give quasi particle displacements in the xz and yz planes respectively. If the material has higher order transversely isotropic symmetry, a point discussed later, then these solutions in the yz plane become pure modes. The second shear mode (S2) has pure displacement in both xz and yz planes and a velocity given by

$$V_{S2} = \sqrt{\frac{I}{\rho}} \tag{2}$$

where in the xz plane of an orthotropic material

$$I = (C_{66}Cos^2\theta + C_{44}Sin^2\theta)$$

and in the yz plane

$$I = (C_{66}Cos^2\theta + C_{55}Sin^2\theta).$$

ULTRASONIC IMPULSE RESPONSE OF CARBON FIBRE LAMINATES

The formulae above predict the velocity with which the wavefront moves forward in the direction of the applied stress. However, in a quasi mode the energy of the ultrasonic wave moves with a group velocity different from the phase velocity of wavefronts. The well known relation [9] between phase velocity ($\underline{Vp}$) and group velocity($\underline{Vg}$) or vice versa is:

$$\underline{V_p} = V_g \, Cos\psi \, \underline{p} \tag{3}$$

where ψ is the angle between the phase and group velocity directions and $\underline{p}$ is a direction of the phase velocity where its magnitude satisfies (3).

In calculating group from phase velocity, we must find ψ. This is accomplished using the appropriate cross-section of a mode's slowness (the inverse of velocity) surface. The direction of energy propagation is along the normal to the slowness surface. Having the calculated phase velocity, its direction ($\underline{p}$) and the direction of energy propagation from the slowness surface, the magnitude of $\underline{V_g}$ satisfying (3) can be found.

In the experiments to be described, it is shown that some observed features travel with the group velocity of the mode, and it is necessary to calculate phase velocity from this data, i.e. we must find the direction $\underline{p}$ from the measured group velocity. Group velocity yields the co-ordinates of points which are moving in phase, and this is parallel to the wavefront direction. Hence, the phase velocity direction is normal to the group velocity surface. Knowing group velocity and phase velocity directions the magnitude of the phase velocity can be calculated from group velocity measurements via equation (3).

3. EXPERIMENTAL METHOD

3.1 Material characterisation

The sample used in the ultrasonic experiments was a 40 ply unidirectional composite (denoted $[0]_{40}$) laminate of 5.5mm thickness made from carbon-epoxy pre-preg (ICI 7716H resin , Enka Tenax HTA fibre in 12K tows).

A set of experiments were performed, to obtain initial values for some of the elastic stiffness constants (C_{ij}) of the material. Tensile, flexural and conventional ultrasonic velocity measurement of 32 layer unidirectional ($[0]_{32}$) and cross-ply ($[0,90]_{16s}$ where [0,90] are the layer directions and the subscript is the number of layers each side of the mid-plane)) samples made with the same pre-preg as the $[0]_{40}$ sample were performed. This gave C_{ij} values shown in Table I for the various methods. The last column of Table I , which was used in calculating velocities from (1) and (2), is the set of constants in which values from conventional ultrasonic tests were used when available and averaged mechanical values in the remaining cases. Material density was found by weighing small samples in air and water giving a figure of 1.54±0.05 gm/cc which is consistent with literature data for this type of material.

ULTRASONIC IMPULSE RESPONSE OF CARBON FIBRE LAMINATES

Elastic constant	Value from tensile E_{ij}	Value from flexural E_{ij}	Ultrasonic value	Initial value
C_{11}	129.3	118.15	116	116
$C_{22}=C_{33}$	9.8	9.46	13.1	13.1
$C_{12}=C_{13}$	4.33	4.19	----	4.26
C_{23}	3.33	3.22	----	3.28
C_{44}	3.23	3.12	3.02	3.18
$C_{55}=C_{66}$	4.2	----	4.4	4.3

Table I Initial elastic stiffness constants calculated from tensile flexural and ultrasonic test data (all values in GPa.)

3.2 Impulse response measurements

The main experiments involved collecting waveforms along a series of directions in the xz and yz planes of the laminate. Fig.2 shows the general configuration for experiments. A broadband capacitance receiver [10] was used in most cases. To operate the capacitance receiver on the insulating epoxy surface of the sample, a 20μm thick brass foil ground plane was adhered to the surface with epoxy resin and polished flat. 5μm thick polymer film was then used to separate the electrodes. A Cooknell amplifier biased the electrodes and amplified the ultrasonic signals arriving at the receiver.

Nd:YAG laser pulses were focussed to a 0.5mm diameter spot on the sample face opposite the receiver. The focussing lens was mounted along with a 45° dielectric mirror on a micrometer-controlled linear stage, an arrangement which allowed the laser pulse to be scanned accurately over the sample surface. Scans on the $[0]_{40}$ laminate were carried out in which the angle (θ) to the surface of the path from source to receiver was changed initially in 1° steps and then reduced to 0.5° and 0.25° to compensate for the large path length changes as the direction approached 10° to the surface. Scans were carried out in the xz and yz planes.

To fully map the velocity of the first arrival, especially for the xz direction, required the separation of source and receiver over the samples full width. In this scan a Panametrics 10MHz , 0.25" diameter compression wave transducer adhered to the sample surface over a small area (2mm diameter) and positioned close to one edge was used as a receiver. This provided waveforms with a higher signal to noise ratio from which more accurate first arrival measurements could be made than was possible with the capacitance receiver. A thin smear of fluid was applied to the surface before firing the laser pulse, to provide a high amplitude normal impulse to the surface. Some ablation of the sample did occur, leaving small pits in

ULTRASONIC IMPULSE RESPONSE OF CARBON FIBRE LAMINATES

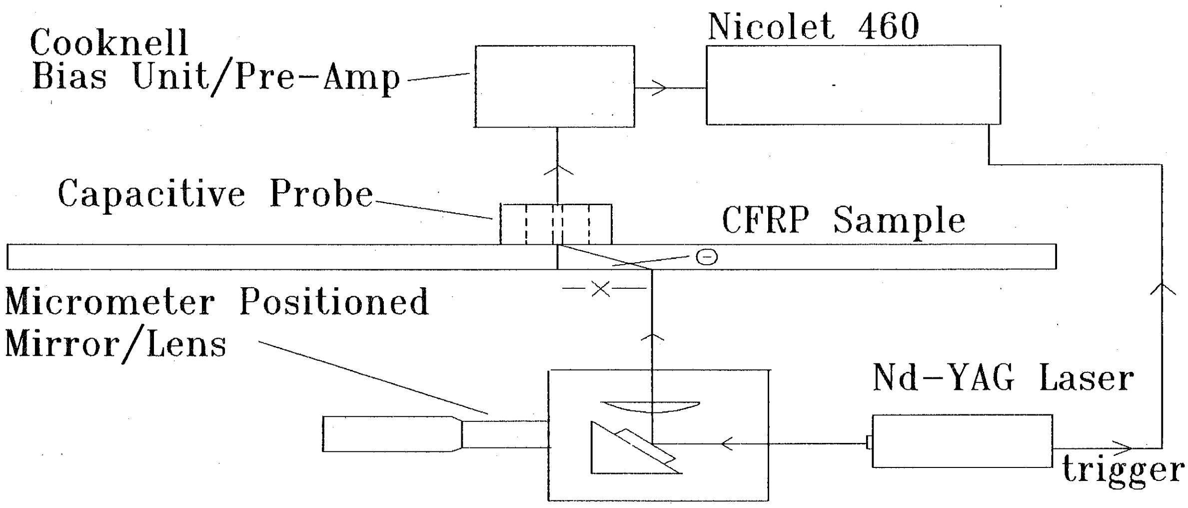

Fig. 2 Experimental equipment used for measurement of impulse response.

its surface. At each source position sixteen waveforms were summed by a Nicolet 460 digital oscilloscope. Later the averaged waveforms were transferred to an IBM PS2/70 for further processing.

4. RESULTS AND DISCUSSION

4.1 Bulk wave velocity measurements

Experimental waveforms collected using the apparatus of Fig.2, for various angles of propagation with respect to the laminate surface (defined by the distance X), were written into a data file suitable for producing waterfall plots. These plots for the xz and yz planes of the $[0]_{40}$ laminate are shown in Figs.3 and 4 respectively.

The waveform at $\theta=90°$ (i.e. on-epicentre with respect to the source) in Fig.3 illustrates the behaviour expected [11,12] for a normal impulse source in an isotropic material. Such waveforms exhibit a monopolar positive longitudinal arrival, followed by a slowly rising section which is followed by a step-like downward shear arrival. This is then followed by a multiple reflection of this basic signal within the laminate thickness. As the source and receiver are separated, and the angle of propagation decreases towards zero (i.e. towards a direction parallel to the laminate surface), the amplitude of the first shear arrival increases and the longitudinal wave gradually falls. By measurement of the arrival time of the start of the signal (labelled A on Fig.3) and the peak (labelled B) indicating the slow shear arrival time and using the calculated distance direct from source to receiver the apparent bulk velocity of these features can be found. These data are shown in Fig.5. Comparison of the measurements to velocities predicted with (1) in the yz plane show the measured velocities to be close to the phase velocities of the longitudinal and the slower shear velocities. Also calculated velocities diverged from the constant velocity trend displayed by the

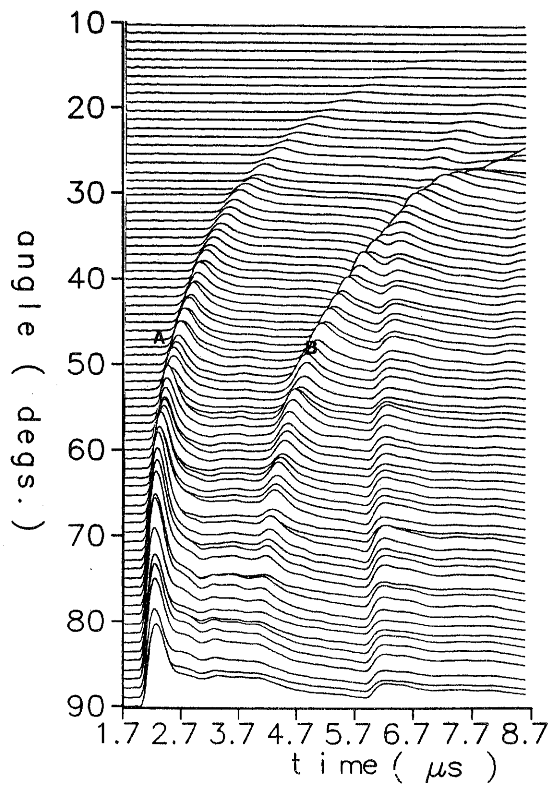

Fig. 3 Waterfall plot of yz plane data.

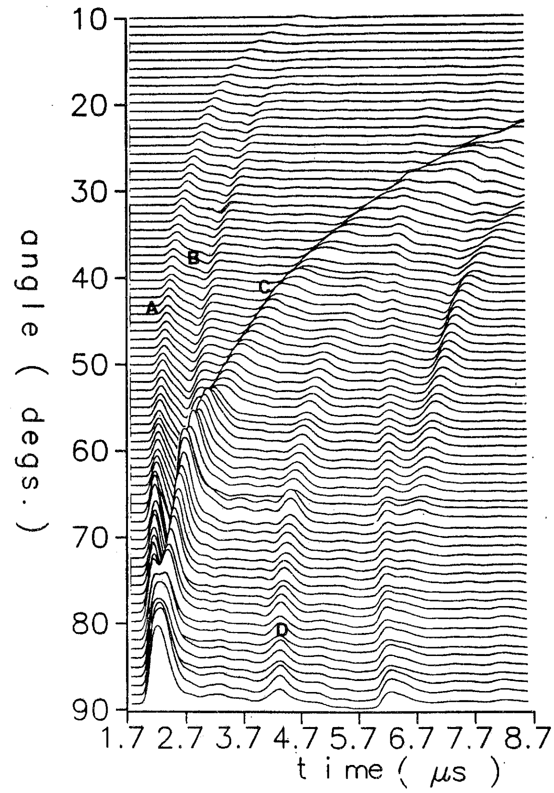

Fig. 4 Waterfall plot of xz plane data.

measurements indicating that some values of C_{ij} in Table I used in the calculation, are incorrect. Some of these were determined from static tests, and it is known that the values of dynamic moduli can differ from their static counterparts.

The detailed (1°) scan in the anisotropic xz plane, as shown in Fig.4, exhibits additional features which were not present in the data taken perpendicular to the fibres in the yz plane. With the receiver on epicentre (90° to the laminate surface) the same waveform as seen in Fig.3 with clearly separated longitudinal and shear arrivals is received. As the source moves away from the receiver (vertically on the diagram) an additional mode becomes visible, present between the longitudinal and slow shear arrivals, which subsequently separates into two branches. Times of first arrival were measured for the four features (labelled A to D on Fig.4), and an estimate made of the experimental bulk velocity of each mode. Comparison with calculated phase and group velocities showed the features to be the quasi longitudinal and shear modes propagating with their group velocities and the pure shear mode propagating with its phase velocity. Note that values of velocity could not be obtained for all features over all angles, as they tended to merge together when the source was close to the receiver, and in addition some were superimposed at angles close to the fibre axis. In this plane the constants of Table I were found to produce calculated velocities

ULTRASONIC IMPULSE RESPONSE OF CARBON FIBRE LAMINATES

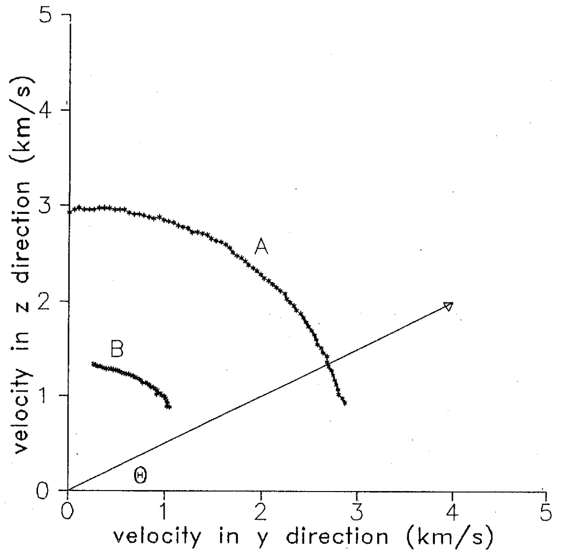

Fig. 5 Velocity of A&B Fig. 3

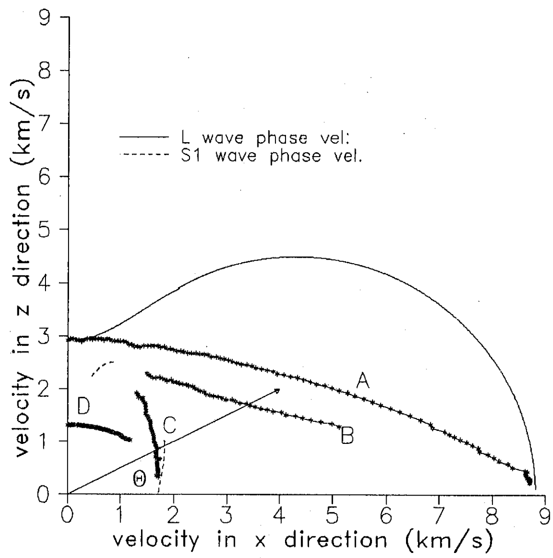

Fig. 6 Velocity of A-D Fig.4 and reconstructed phase velocity of A-C

which more closely resembled the measured velocity data.

From the discussion above, we can identify and measure the velocity of propagation of the major first features generated by an ablative laser ultrasonic source in unidirectional CFRP. The capacitive transducer proved essential in recording an accurate representation of this situation but the relatively low signal to noise ratio of the detector makes it difficult to measure the time of first arrival with high accuracy when propagating over long path lengths. By repeating the experiment with the piezoelectric detector described earlier, velocity measurements of the first (longitudinal) arrival time could be improved greatly. Combining this with the data for the shear modes gives the velocity data of Fig.6 (over the widest angular range possible in this sample).

In Fig.4 it is observed that the two branches (B and C) of the quasi-shear mode come together as the direction approaches 90° which is predicted by group velocity calculations but instead of stopping as suggested by the theory they continue in a single feature whose velocity reaches that of the longitudinal wave on epicentre. Such behaviour points to the anisotropic material producing additional shear components from a point, normal force not observed in isotropic media or anticipated by the calculation.

4.2 Calculation of elastic stiffness constants

The velocity data for marked features in the yz and xz planes were used in the following analysis to estimate the C_{ij} of the material, with no *a priori* knowledge of their values before

ULTRASONIC IMPULSE RESPONSE OF CARBON FIBRE LAMINATES

performing the analysis. First, for the quasi modes in the xz plane, polynomial equations of differing orders were least squares fitted to the measured data. The phase velocity of the measured data could then be found, using these polynomial fits and equation (3). This involved finding the normal to the polynomial form of the group velocity surface to give the appropriate direction for the phase velocity, and calculating the component of the group velocity (the magnitude of the phase velocity) in this direction. This process led to the reconstructed phase velocity data, shown in Fig.6, for quasi modes in the xz plane . Note that as for the experimental data, the reconstructed phase velocity surfaces for the quasi-longitudinal and quasi-shear modes were of limited angular range. For the pure shear mode, (D) the group and phase velocities are the same.

Squaring and adding the quasi solutions of equation (1) for the xz plane and substituting for $\cos\theta$ in terms of $\sin\theta$ gives a relation which can be fitted to the sum of the measured velocities squared. Squaring, subtracting and squaring the same quasi solutions gives an equation which can be fitted to the same combination of the measured velocity. Coefficients of the terms in these fits are functions of the elastic constants and can be used to calculate elastic constants as detailed in Table IIa. The obviously poor value of C_{13} obtained from the $\sin^4\theta$ term indicates that this term was not very significant in refining the fit to the experimental data. Further values of C_{66} and C_{44} can be obtained from fitting the measured velocity for the pure shear mode to equation (2) which has been manipulated in similar way to the quasi mode equations.

In the yz plane, the solutions predicting the measured surfaces are again those from equation (1). These solutions can be simplified as the uniformity of velocity with direction in this plane shows the material to be transversely isotropic giving some simplification ($C_{33}=C_{22}, C_{12}=C_{13}, C_{44}=(C_{33}-C_{23})/2, C_{55}=C_{66}$) of the elastic constants in (1). Manipulating the solutions in the same fashion as in the xz plane gives equations which are constant with direction. Fitting the measured sum and difference data values with direction to a constant gives two equations which can be solved for the additional values of C_{22} and C_{44} shown in Table IIb.

After using the velocity information to deduce elastic constant values in both directions it is possible to use averaged values from Table II to predict theoretically the angular variation in velocity for the xz and yz plane. Good agreement was found between such predictions and the measured data. It is interesting to note that the values of elastic constants derived from the laser generated ultrasound experiment differ somewhat from the values obtained via standard mechanical testing. The largest of these is the difference in the value of C_{23}, given as 3.27±0.05 GPa by mechanical testing in Table I, and 8.74 GPa when calculated from C_{33} and C_{44} ($C_{23}=C_{33}-2C_{44}$). So the higher C_{23} value is the result of much higher and slightly lower experimental laser ultrasonic values than mechanical values for C_{33} and C_{44} respectively. A difference of 400 m/s in the longitudinal wavespeed across the fibres is produced by this shift in C_{33}. It appears from this that the mechanical test elastic constant

Least squares fit to	Terms used from fit	Additional C_{ij} required	C_{ij} calculated	Value of C_{ij} (GPa)
sum & diff.	constant	------------	C_{11}	119.58
sum & diff.	constant	------------	C_{55}	4.59
sum	$Sin^2\theta$	C_{11}, C_{55}	C_{33}	14.35
diff.	$Sin^2\theta$	C_{11}, C_{55}, C_{33}	C_{13}	5.83
diff.	$Sin^4\theta$	C_{11}, C_{55}, C_{33}	C_{13}	-0.30
pure shear	constant	-----------	C_{66}	4.44
pure shear	$Sin^2\theta$	-----------	C_{44}	2.61

Table IIa Values of elastic stiffness constants calculated from least squares fit to phase velocity data in xz plane.

Least squares fit to	C_{ij} calculated	Value of C_{ij} (GPa.)
sum & diff.	C_{22}	14.08
sum & diff.	C_{44}	2.87

Table IIb Values of elastic stiffness constants calculated from least squares fit to phase velocity data in yz plane.

values do not reproduce accurately the behaviour of the ultrasonic modes, particularly that of the compression wave. Why C_{33} should be so much further away from the range of the mechanical test values deserves further investigation. Reasons postulated include the different type and rate of change of the loads applied by ultrasonic and mechanical tests or the possibility of microcracks in the material opening up under the strain of the mechanical testing.

5. CONCLUSIONS

The data we have taken shows that when close to the source the response of a unidirectional CFRP laminate can readily be understood in terms of discrete pulses of bulk modes, predicted by theory for propagation in a given direction. This is shown most clearly by the detailed scans of the $[0]_{40}$ laminate, and in particular the velocity data of the major features and the analysis to derive the C_{ij} values.

Reconstruction of the bulk wave phase velocity surfaces using the mathematically and computationally simple method described proved possible with the quality of data taken in these experiments. Values of C_{ij} derived from the analysis were able to reproduce accurately the ultrasonic behaviour, whereas values derived from mechanical testing were less able to do so. The reasons for the discrepancies would form a possible area of further investigation.

6. REFERENCES

[1] R.M.White, J. Appl. Phys., 34 pp3559-3567 (1963).

[2] A.Askar'yan, A.Prokhorov, G.Chanturia & M.Shipulo, Sov. Phys. JETP, 17 pp1463-1465 (1963).

[3] D.A.Hutchins, in *Physical Acoustics*, edited by W.P.mason and R.N.Thurston, Vol.XVIII, pp1-123, (Academic Press, Boston, 1988).

[4] C.B.Scruby & L.E.Drain, *Laser Ultrasonics-Techniques and Applications*, (Adam Hilger-IOP Publishing Ltd., Bristol, 1990).

[5] B.Castagnede, W.Sachse & M.O.Thompson, in *Proc. Ultrasonics International 89*, pp71-77, (Butterworth-Heinemann, London, 1990).

[6] A.Every & W.Sachse, Phys. Rev. B, Vol.42 (13) pp8196-8205 (1990).

[7] K.Kim, W.Sachse & A.Every, Jour. Acoust. Soc. America, Vol.93(3) pp1393-1406 (1993).

[8] M.J.P.Musgrave, Proc. R. Soc. London, A226 p339 (1954).

[9] E.G.Henneke,II, Jour. of Acoust. Soc. Am., Vol.51 pp210-2177 (1972).

[10] W.Sachse & N.N.Hsu, in *Physical Acoustics*, edited by W.P.Mason and R.N.Thurston, Vol. XIV pp277-406, (Academic Press, New York, 1979).

[11] Y.H.Pao & A.N.Ceranoglu, J. Appl. Mech., Vol.48 pp125-147 (1981).

[12] J.E.Sinclair, J. Phys. D:Appl. Phys., Vol.12 pp1309-1315 (1979).